ICE ACCRETION SIMULATION IN PRESENCE OF A HOT AIR ANTI-ICING SYSTEM

Carlos N. Donatti, newmar@sinmec.ufsc.br
Rafael A. Silveira, rafael_silveira1978@hotmail.com
Gerson Bridi, gerson@sinmec.ufsc.br
Clovis R. Maliska, maliska@sinmec.ufsc.br
António F. C. da Silva, afabio@sinmec.ufsc.br
Departamento de Engenharia Mecânica – UFSC, Caixa Postal 476, 88040-000, Florianópolis-SC, Brasil

Abstract. *This work presents two numerical models to simulate ice accretion with hot air anti-icing systems. The first model, called "1D Normal", assumes that there is heat flux just in the surface normal direction and the heat flux is modeled using the electrical analogy. The second model assumes that there is heat flux also in the surface direction, this model is called "1D Surface". However, this model neglects the temperature gradient in the normal direction, therefore, every layer has the same temperature for a given position. The anti-icing system acts only in a part of the inner wing, with the non-protected region modeled as adiabatic wall or as semi-infinite solid, being the later the alternative used for ice accretion problems when no anti-icing systems are considered. The surface temperature obtained with these formulations agree well with numerical results from Lewice code.*

Keywords*: Aircraft ice accretion, anti-icing systems, hot air systems and Piccolo tube.*

1. INTRODUCTION

Two usual ways to prevent ice accretion on the leading edge of aerodynamic profiles are by using anti-ice and de-icing systems. Among these systems the most important ones are those which employ electric resistors and hot air. The later is the most common on today's commercial aircrafts. The main component of the hot air system is a tube, usually known as Piccolo tube, which is located just behind the leading edge along the wingspan wise. This tube possesses orifices to blow hot air, from the airplane engine, on the leading edge. The heat diffuses itself on the wing and prevents the impinging water to freeze.

The design parameters of a hot air anti-ice system, i.e., hot air temperature and mass flow, number, position and diameter of the orifices may be obtained as a result of computer simulations which involve energy and mass balances inside and outside of the wing. There are several software used to simulate icing prevention systems, among them Lewice (Wright, 1995 and 2003) is the most known. This software in its initial versions (Wright, 1995) has implemented a one-dimensional model in order to simulate electro thermal and hot-air systems. In the later versions (Wright, 2003), a more complex two-dimensional model was introduced. In these versions the heat conduction is solved both in the wing and in the ice layers, coupled with the thermodynamic model of ice accretion.

In this paper two kinds of one-dimensional models to simulate hot air systems are presented, namely 1D Normal and the second 1D Superficial. They are described in details in the next sections.

2. ICE ACCRETION MODEL

The main goal of anti-icing systems is to have a surface temperature high enough to prevent ice formation. The surface temperature for both hot-air anti-icing formulations is obtained from an energy balance. This energy balance is illustrated in Fig. 1 and given by

$$q_o + q_{s,imp} + q_{ke,ar} + q_{ke,água} + q_{lat} + q_{evap} + q_{conv} + q_{s,\,flow} = 0\,, \tag{1}$$

where

q_{lat} - heat gained for phase changes;

q_{evap} - heat release by evaporation;

$q_{ke,ar}$ - heat gained for kinetic heating from air;

$q_{ke,imp}$ - heat gained for kinetic heating from the impinging water droplets;

$q_{s,imp}$ - heat gained or released for a given temperature change, from the impinging water droplets;

$q_{s,\,flow}$ - heat gained or released for a given temperature change, from the runback water;

q_{conv} - convection heat given by temperature gradient between surface and air outside boundary layer;

q_o - conduction heat given by anti-icing system.

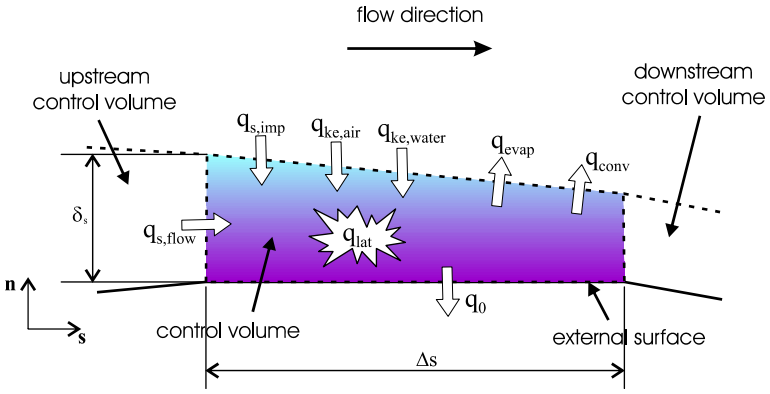

Figure 1. Heat balance.

Surface temperature (T_s) for each control volume is the unknown in Eq. (1) which can be written as $f(T_s) = 0$. The physical significance of each term in the energy balance can be found in Silveira (2001), Silveira and Maliska (2001) and Wright (1995), except for the term q_o. In Silveira (2001), the thermodynamics model is described for non-protected surfaces; therefore this term is modeled by a conduction heat flux in a semi infinite solid. As this work considers an anti-icing system, the conduction heat flux is given by the anti-icing system and is detailed in next sections for both formulations.

The other balance for the ice accretion model is a mass balance. The mass balance for the control volume shown in Fig. 2 can be written as

$$\dot{m}_{imp} + \dot{m}_{rb,in} = \dot{m}_{evap} + \dot{m}_{rb,out} + \dot{m}_{shed} + \dot{m}_{freeze} \tag{2}$$

where

$\dot{m}_{imp}$ - impingement water flux;

$\dot{m}_{rb,in}$ - runback water flux from the upstream control volume;

$\dot{m}_{evap}$ - evaporation water flux;

$\dot{m}_{rb,out}$ - mass flux of no freezing water;

$\dot{m}_{shed}$ - water shedding, due to aerodynamic force;

$\dot{m}_{freeze}$ - freezing water rate.

The expression from these terms can be also found in Silveira (2001), Silveira and Maliska (2001) and Wright (1995).

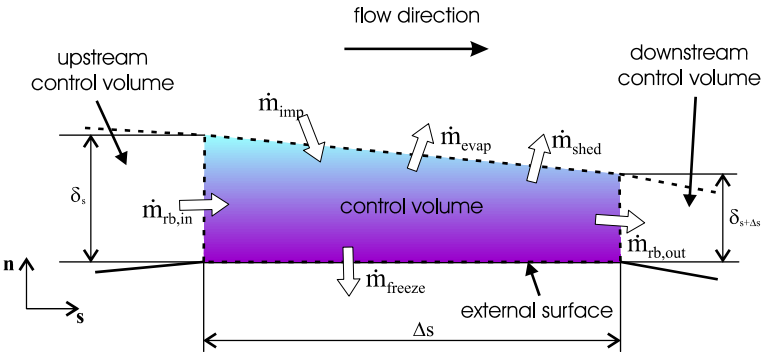

Figure 2. Mass balance.

3. "1D NORMAL" FORMULATION

In this formulation it is considered that there is no heat flux in the tangential direction. The problem is, therefore, modeled as a one-dimensional problem for each discretized position along the surface using the electrical analogy.

Figure 3 illustrates the energy balance for a hot air anti-icing system. In this figure the airfoil is composed by three different materials with different thermodynamic properties, and the ice layer is also considered. The forced convection into the airfoil is modeled by an internal convection coefficient h_{ai} and an internal temperature $T_{\infty,i}$ is considered a known. The electrical analogy is employed and the heat flux from anti-icing system, for a given position, is represented by

$$q_0'' = \frac{T_{\infty,i} - T_s}{R_{tot}} \tag{3}$$

where R_{tot} is the equivalent thermal resistance, given by

$$R_{tot} = \frac{1}{h_{ai}} + \frac{L_1}{k_1} + \frac{L_2}{k_2} + \frac{L_3}{k_3} \tag{4}$$

where k_i is the thermal conductivity and L_i is the layer thickness for each material.

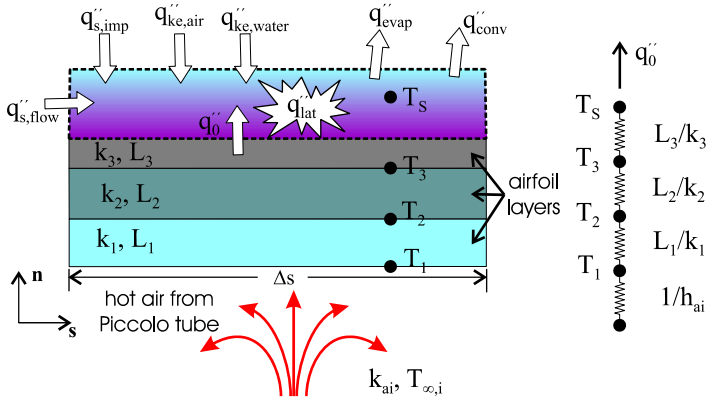

Figure 3. Electrical analogy.

Equation (3) can be rewritten as

$$q_0 = \frac{T_{\infty,i} - T_s}{\frac{1}{h_{ai}} + \sum_{i=1}^{n} \frac{L_i}{k_i}} \Delta s \Delta y \tag{5}$$

where “n” is the number of materials which form the airfoil. This heat flux needs to be inserted in the energy balance given by Eq. (1).

4. “1D SURFACE” FORMULATION

This model considers the existence of temperature gradient only in the tangential direction, that is, each tangential position has a single temperature for every airfoil layer. This hypothesis is good for airfoil materials with high thermal conductivity. Figure 4 shows the energy balance for this formulation.

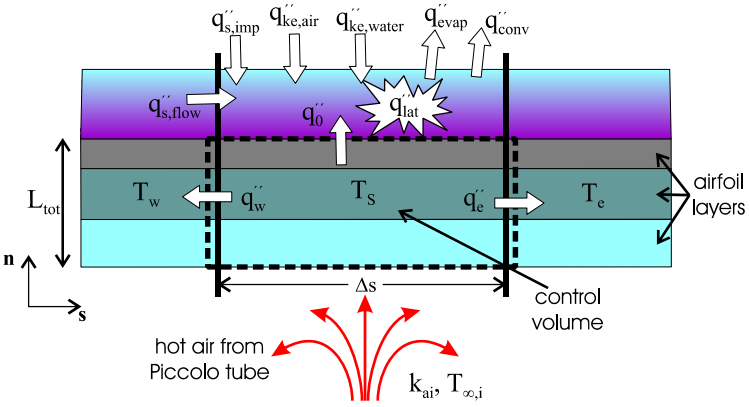

Figure 4. Heat balance for "1D Surface" formulation.

The energy balance shown in Fig. 4 can be written by

$$q''_{ai}\Delta s\Delta y - q''_{w}L_{tot}\Delta y - q''_{e}L_{tot}\Delta y - q''_{o}\Delta s\Delta y = 0 \tag{6}$$

where L_{tot} is the material total thickness and q''_{ai} is the heat flux from anti-icing system, given by

$$q''_{ai} = h_{ai}\left(T_{\infty,i} - T_s\right) \tag{7}$$

The diffusive flux in surface direction can be calculated as

$$q''_{w} = k_{eq}\cdot\frac{T_s - T_w}{0,5\cdot(\Delta s_w + \Delta s)} \tag{8}$$

$$q''_{e} = k_{eq}\cdot\frac{T_s - T_e}{0,5\cdot(\Delta s_e + \Delta s)} \tag{9}$$

where k_{eq} is the equivalent thermal conductivity given by

$$k_{eq} = \frac{\sum_{i=1}^{n} L_i\cdot k_i}{\sum_{i=1}^{n} L_i} \tag{10}$$

Inserting Eq. (8) and (9) in energy balance given by Eq. (6) and rearranging terms, q_0 can be expressed by

$$q_0 = 2k_{eq}L_{tot}\Delta y\left(\frac{T_w - T_s}{\Delta s_w + \Delta s} + \frac{T_e - T_s}{\Delta s + \Delta s_e}\right) + h_{ai}\left(T_{\infty,i} - T_s\right)\Delta s\Delta y \tag{11}$$

The first term in the right-hand side of Eq. (11) represents the heat flux in the tangential direction. As in the previous formulation, Eq. (11) is used in energy balance given by Eq. (1).

5. HEAT FLUX IN NON-PROTECTED REGIONS

Usually only the wing leading edge is protected by a heating system (sometimes the nacelle is also protected), as shown in Fig. 5. Therefore when the heating system is operating, only in the heated part is applied the convection boundary conditions. On the unprotected region there are two common possibilities of boundary conditions. The original one presented by Messinger (1953) considers an adiabatic surface, and the semi-infinite solid condition implemented in Lewice (Wright, 1995).

In this work the adiabatic condition is used setting the convection heat transfer coefficient to zero at the unprotected part of the surface.

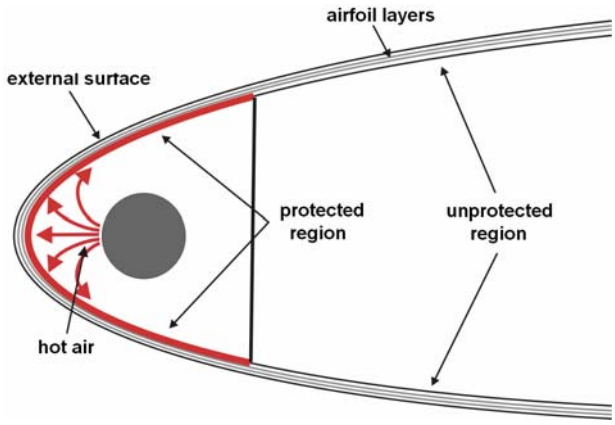

Figure 5. Cross-section of Piccolo tube anti-icing system.

6. VALIDATION OF THE ANTI-ICING SYSTEM

Data available in Wright (2004) were used to validate the formulations presented herein. They are summarized on Tab. 1. The inner airfoil boundary condition applied is convection. A reference temperature and the convection heat transfer coefficient were obtained from Wright (2004). It is important to highlight that the internal convection heat transfer coefficient profile was obtained by numerical simulations, using Lewice (Wright, 2004), as well as the reference external temperature. The wing material is 3.175 mm thick with a conductivity of 176.53 W/m K.

Table 1. Ice accretion conditions for validation case.

Ice accretion conditions	
Profile	NACA 23014
Chord (m)	1,52
AOA (°)	3
V_∞ (m/s)	59,16
T_∞ (K)	267,8
P_∞ (kN/m^2)	101,3
MVD[1] (µm)	29
LWC[2] (g/m^3)	0,87
T_{ai} (anti-icing) (K)	450
Total time (min)	22,5

As discussed, the Piccolo tube has arrays of orifices to blow small jets of hot air. Since the orifices are not all aligned, three cut-sections were analyzed: a) coincident with one jet, b) coincident with two jets and a c) between jets. In Fig. 6 these three situations are depicted. The combination of these three distributions and the conduction heat transfer models lead to 6 cases.

In the next sections the simulated cases are presented. They are grouped according to the section and the respective convection heat transfer coefficient. The results are presented for each coefficient profile. The outside temperature profile is shown for both formulations, as well as the resulting residual ice shapes.

[1] MVD – Median volume droplet diameter
[2] LWC – Liquid water content

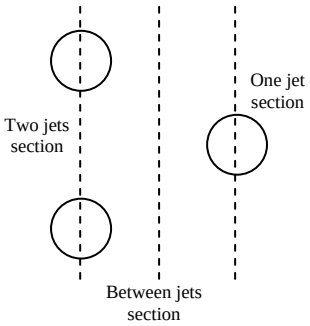

Figure 6. Selected wingspan positions for anti-icing system.

6.1. Section between jets

Figure 7 shows the internal convection coefficient at section between jets.

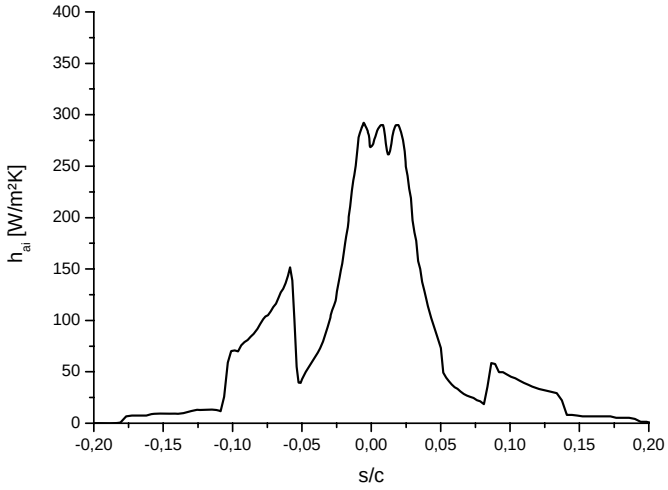

Figure 7. Internal convection coefficient at between jets section.

The simulation results are presented in the next pictures. Figure 8 depicts the temperature distribution on the external surface and Fig. 9a and 9b show the residual ice shapes resulting from both formulations.

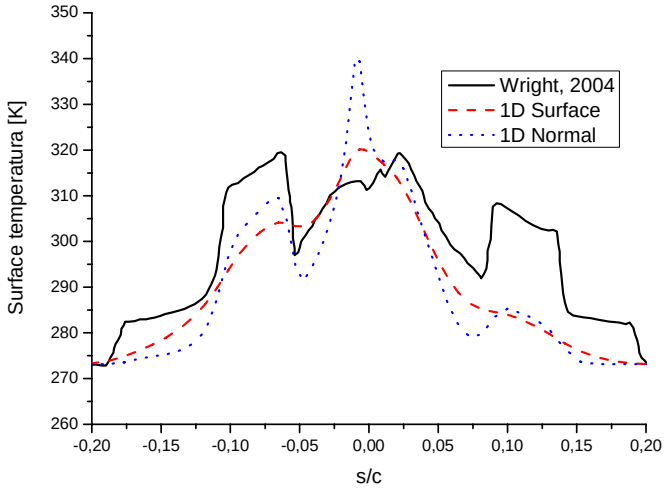

Figure 8. External temperature variation at between jets section.

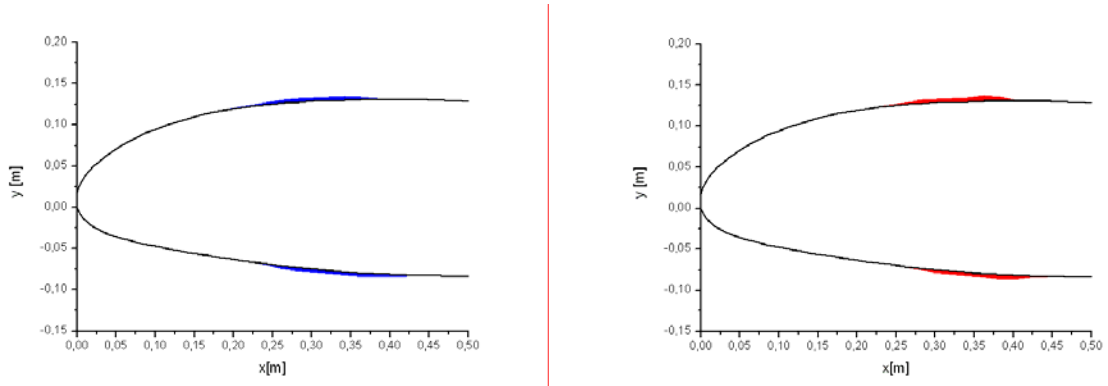

(a) (b)

Figure 9. Residual ice shapes for section between jets: (a) “1D Normal” e (b) “1D Surface”.

6.2. Section crossing one jet

Figure 10 shows the internal convection coefficient at section crossing one jet.

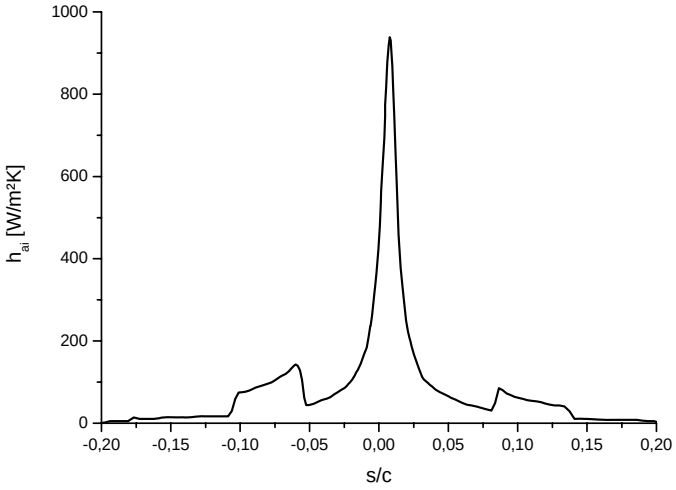

Figure 10. Internal convection coefficient at one jet section.

The results obtained for the single jet section are depicted on Fig. 11, 12a e 12b.

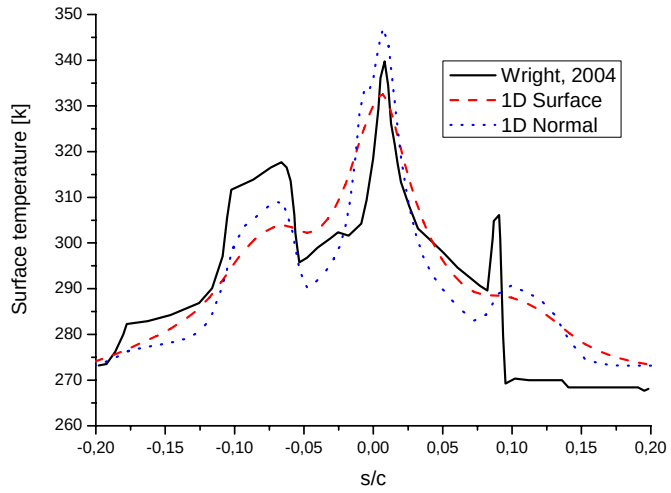

Figure 11. External temperature variation at one jet section.

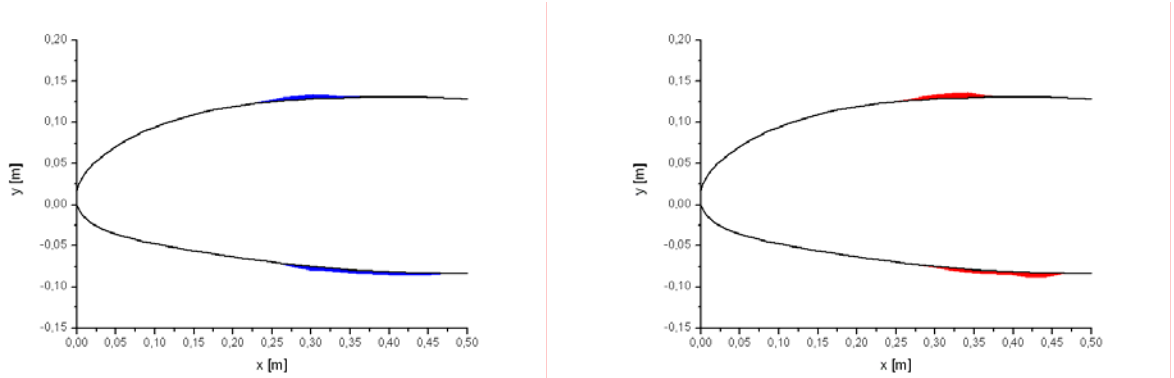

(a) (b)

Figure 12. Residual ice shapes for one jet section: (a) “1D Normal” e (b) “1D Surface”.

6.3. Section crossing two jets

Figure 13 shows the internal convection coefficient at section crossing two jets, while Figures 14, 15a and 15b show the surface temperature and the residual ice accreted for this section.

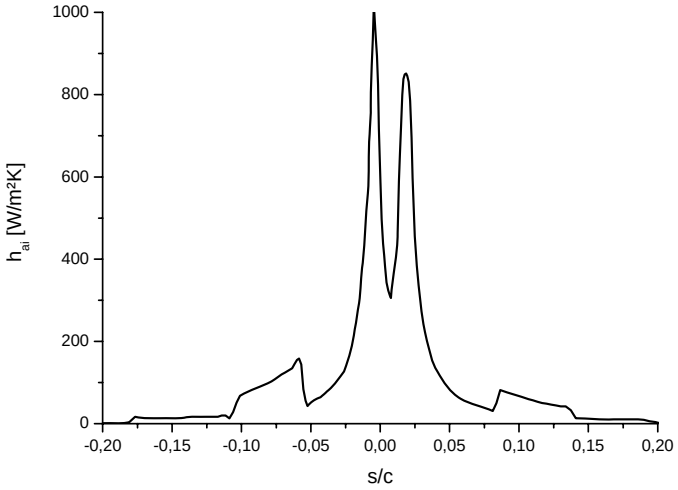

Figure 13. Internal convection coefficient at two jets section.

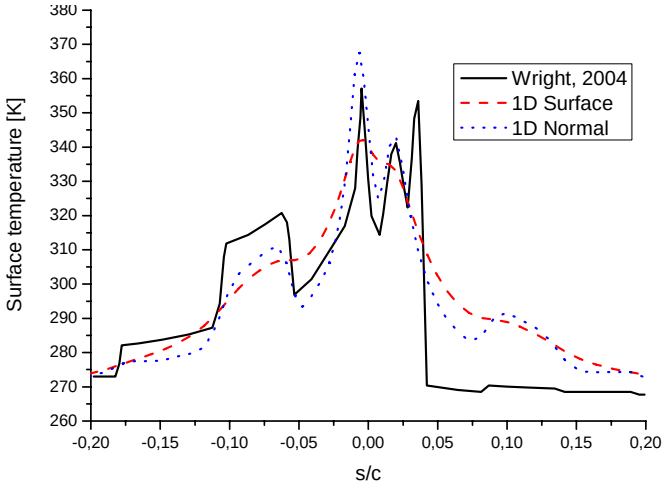

Figure 14. External temperature variation at two jets section.

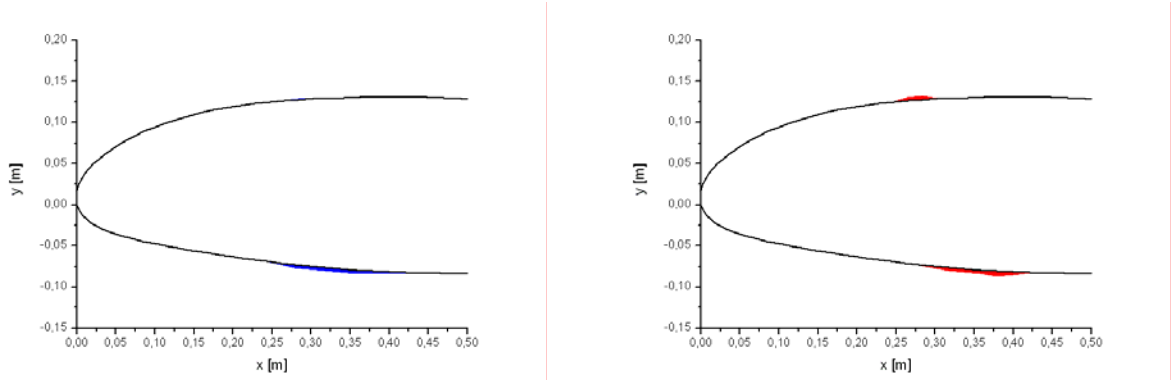

(a) (b)

Figure 15. Residual ice shapes for two jets section: (a) “1D Normal” e (b) “1D Surface”.

To point out the importance of the anti-icing system, Fig. 16 shows the ice accreted for the conditions show in Tab. 1 if no anti-icing system is provided.

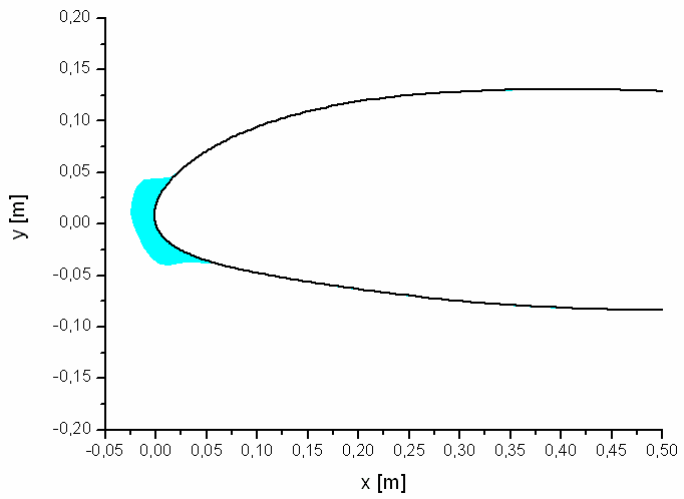

Figure 16. Ice accretion without anti-icing system.

7. CONCLUDING REMARKS

This paper presented two methodologies for simulating ice accretion with anti-icing systems. They employ the thermal resistance concept applied in the normal and tangential directions. Both revealed to be good alternatives for engineering calculation of anti-icing systems it was shown that the “1D Normal” model presents high temperature gradients in the tangential direction, being able to better represent the temperature peaks. In the other hand, the temperature profiles obtained with the “1D Surface” model have smooth gradients, because this formulation considers conduction heat flux in the tangential direction.

When compared with Lewice code (Wright, 2004), in cut-section cases with one and two impingement jets – Fig. 11 and 14, respectively – “1D Normal” model obtain the best results, because those cases present high temperature gradients. For the cut-section between jets, the “1D Surface” model, see Fig. 8, presented good results near stagnation point.

An interesting fact can be noted in external temperature profile for the case with two impingement jets. In Fig. 14 the Lewice code presents an external temperature profile with three peaks, while results obtained with models proposed in this work captured two peaks. One can speculated that the results obtained with “1D Normal” and “1D Surface” formulations are physically consistent, since the internal convection heat transfer coefficient, shown in Fig. 13, also shows two peaks.

8. ACKNOWLEDGEMENTS

The authors want to acknowledge the partial support of CAPES (Coordenação de Aperfeiçoamento de Pessoal de Nível Superior) and Embraer (Empresa Brasileira de Aeronáutica S.A.).

9. REFERENCES

Silveira, R. A., 2001, "Simulação Numérica da Formação de Gelo na Borda de Ataque de Perfis Aerodinâmicos", MsC Thesis, Federal University of Santa Catarina, Florianópolis, SC, Brazil, In Portuguese.

Silveira, R. A., 2006, "Previsão Tridimensional da Formação de Gelo em Perfis Aerodinâmicos", Dr. Thesis, Federal University of Santa Catarina, Florianópolis, SC, Brazil, In Portuguese.

Silveira, R.A, Maliska, C.R, 2001, "Numerical Simulation of Ice Accretion on the Leading Edge of Aerodynamic Profilies", Proceedings of the 2nd International Conference on Computational Heat and Mass Transfer, Rio de Janeiro, RJ, Brazil.

Wright, W. B, 1995, "Users Manual for the Improved NASA Lewis Ice Accretion Code Lewice 1.6", NASA CR – 198355.

Wright, W. B., 2003, "User's Manual for the NASA Glenn Ice Accretion Code Lewice Version 3.0", available on Lewice 3.0 release CD.

Wright, W. B., 2004, "An Evaluation of Jet Impingement Heat Transfer Correlations for Piccolo Tube Application", AIAA Paper 2004-0062.

10. RESPONSIBILITY NOTICE

The authors are the only responsible for the printed material included in this paper.